

specification in such a way as to reasonably convey to one skilled in the art that the inventor had possession of the claimed invention.

Specifically, the Examiner argues that insertion of the limitation “above -80 degrees C” and “0 degrees C or above” have no support in the specification as filed. Examiner also argues that insertion of the phrase “without freezing (ice formation)” does not appear to have literal support in the generic portion of the specification. Examiner concedes that insertion of the term “vitrifying” upon reconsideration is not considered to be new matter and thus does not have to be addressed in the present response.

Applicant respectfully wishes to address in full each of Examiner’s rejections referenced above. Furthermore, Applicant respectfully asserts that claims 1, 4-10, 12-16, 25 and 26 are fully supported by the specification as filed and therefore comply with the written description requirements of 35 U.S.C. § 112, first paragraph.

Applicant respectfully states that the limitation “above -80 degrees C” and “0 degrees C or above” are selected because these temperatures are mostly used for storage and transportation of biologicals with dry ice (at -80 degrees C), or with ice (0 degrees C). Because other temperatures that are above -196 degrees C (liquid nitrogen boiling point) practically are not of interest we believe that selection of these temperatures is essential and is fully supported by the specification as filed, by the references incorporated therein, and by common knowledge in the art.

Furthermore, Applicant respectfully states that insertion of the phrase “without freezing (ice formation)” does not introduce new matter and is fully supported and described in the specification as filed. To vitrify or to perform the process of vitrification, as that term is uniformly defined in the art and further described in the specification as filed, ultimately necessitates the step of cryopreservation of a sample in such a way that no freezing-induced crystallization or ice formation is caused. This crucial distinction between vitrification method of cryopreservation and simple freezing is repeatedly illustrated throughout the specification as filed, including but not limited to paragraphs 4, 22, 23, and 24 of the specification. Therefore, the phrase “without freezing

(ice formation)” simply reiterates the meaning and limitations of the term “vitrification” as that term is presently defined in the art of cryopreservation. Therefore, Applicant respectfully states that no new or indefinite matter was introduced by insertion of the phrase “without freezing (ice formation)”. This terminology is well known in the art.

In light of the above remarks, Applicant respectfully requests the Examiner to withdraw the rejection of claims 1, 4-10, 12-16, 25 and 26 under 35 U.S.C. § 112, first paragraph.

Rejections of the Claims under 35 U.S.C. § 112, second paragraph

Claims 1, 4-10, 12-16, 25 and 26 were rejected under 35 U.S.C. § 112, second paragraph, for allegedly being indefinite for failing to particularly point out and distinctly claim the subject matter which applicant regards as the invention. Specifically, Examiner stated that in claim 1, step (a), the term “concentrated” is used. Examiner further stated that the term “concentrated” is a term of comparison without a reference point and is, therefore, without distinct metes and bounds, which allegedly renders the claim indefinite.

Examiner further stated that claim 1 has parenthetical insertions which may or may not be intended to further limit the claim. Therefore, Examiner stated that the use of such parenthetical insertions allegedly renders the claims indefinite.

Applicant respectfully wished to address in full each of Examiner’s rejections referenced above. Furthermore, Applicant respectfully states that the limitations of each of the claims listed above are fully defined by the specification as filed and therefore claims 1, 4-10, 12-16, 25 and 26 fully comply with all requirements of 35 U.S.C. § 112, second paragraph.

Applicant alerts the Examiner to the fact that the metes and bounds of the term “concentrated”, as that term is used in claim 1 and dependent claims, are fully defined by

the present specification as filed. Specifically, the concentration of non-permeating co-solutes is defined in paragraph 38 of the specification to be in the 0.1-0.6 mol/l range, and the concentration of permeating cryoprotectant is defined in paragraph 39 of the specification to be above 40 percent-by-weight range. It is important to mention that in the scope of the application a solution is called concentrated if it does not freeze (no ice forms) and vitrifies during cooling to -196°C . It is well known that it is practically impossible to avoid formation of ice during cooling to -196°C if concentration of a solution is below 40% (60% water). For this reason, by default, the cryovitrification process requires using concentrated solutions. It is very known to everybody skillful in the art of cryopreservation (by freezing, or by cryovitrification)

Applicant amended claim 1 to remove the parenthetical insertion “(ice formation)”, therefore Examiner’s rejection of claim 1 because of the parenthetical insertion is believed to be fully addressed by the amendment.

In light of the above remarks and amendments, Applicant respectfully requests the Examiner to withdraw the rejection of claims 1, 4-10, 12-16, 25 and 26 under 35 U.S.C. § 112, second paragraph.

Rejections of the Claims under 35 U.S.C. § 102(e)

Claims 1, 4-7, 9, 10, 12-16, 25 and 26 were rejected under 35 U.S.C. § 102(e) as allegedly being clearly anticipated by US Patent No: 5,800, 978 (“Goodrich et al.”).

Following recent phone conversation with Examiner SAUCIER Applicant respectfully ask the Examiner to consider the difference between Tg and Tg’ (TG-prime) that is clearly explained in the articles (Hatley and Franks, 1991; and Levine and Slade, 1989) enclosed in the letter. During the phone conversation the Examiner agreed that understanding the difference between Tg and Tg’ is very important for proper evaluation of the invention.

Tg is the temperature at which a solution transforms to the glass state during cooling without formation of crystallized phase (i.e. ice). Tg is a function of the solution

concentration. For example, Tg of pure sucrose (100%) is about +60 degrees C, Tg of 10% sucrose solution in water is about -140 degrees C (please see the articles enclosed). At the same time Tg' does not depend on the concentration of the solution. Tg' is the temperature at which solution remaining unfrozen between ice crystals vitrifies during freezing. According to Hatley and Franks (1991) for sucrose dissolved in water Tg' is minus 33 degrees C.

CONCLUSION

In view of the foregoing arguments, Applicant respectfully submits that claims 1, 4-10, 12-16, 25 and 26 satisfy the requirements of 35 USC §§ 112 first paragraph, 35 U.S.C. § 112 second paragraph, and 102(e). Accordingly, Applicants respectfully request reconsideration and withdrawal of these rejections and request that the claims be allowed.

Present amendment and response under 37 C.F.R. § 1.121 is filed in a timely manner prior to expiration of statutory three month period for response, hence no extension fees are believed to be necessary.

Respectfully submitted,

Victor Bronshtein

Inventor

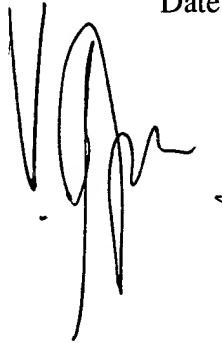
5008 Almondwood Way

San Diego, CA 92130

Email: victorb@ustsd.com

Phone number: 858-245-9323

Date: March __20__, 2006

A handwritten signature in black ink, appearing to be 'Victor Bronshtein', written over a horizontal line.

RESPONSE TO THE LETTER BY SIMATOS, BLOND, AND LE MESTE ON THE RELATION BETWEEN
GLASS TRANSITION AND STABILITY OF A FROZEN PRODUCT

Harry Levine and Louise Slade

Nabisco Brands, Inc., Fundamental Science Group, P.O. 1943, East Hanover, New
Jersey, 07936-1943, U.S.A.

We thank Simatos, Blond, and Le Meste for their Letter to the Editor of Cryo-Letters (1), in which they commend the contribution of the conceptual "food polymer science" approach to problems in the field of food science and technology, as described in our recent review of cryostabilization technology (2). We also thank them for their constructive criticisms of our paper (2), and wish to take this opportunity to respond to their Letter.

Simatos et al. (1) suggest that certain "questions" or "contradictions", relating to interpretation of low-temperature differential scanning calorimetry (DSC) thermograms and identification of glass transitions in thermograms for frozen food materials, "are never discussed" in our papers. We are surprised, since we have addressed these issues extensively in manuscripts (3-5) that preceded the Cryo-Letters review (2) and in two subsequent papers (6,7), for which preprints were shared with Simatos et al. in informal correspondence that preceded submittal of their Letter to Cryo-Letters.

With regard to the ease of identification of glass transitions in DSC thermograms of food materials at low temperature, we have shown (2, Fig. 3) that a real-time analog derivative feature of a DuPont calorimeter provides an amplified profile that benefits from a horizontal baseline with lower noise and greater reproducibility than the baseline of the corresponding primary heat flow curve, in addition to its inherent enhanced capability to reveal multiple, superimposed thermal events. We suggested (3) that use of a derivative profile with such a superior baseline allows unambiguous deconvolution of the characteristic sequential subzero transitions that occur during warming and non-equilibrium melting of frozen aqueous solutions of non-crystallizing solutes (8) and facilitates deconvolution of the more complicated thermal profiles of readily-crystallizable solutes (6). Identification of the salient subzero transition occurring at T_g' (8-10) as the particular glass transition of the maximally freeze-concentrated, amorphous solute/unfrozen water (UFW) matrix surround-



ing the ice crystals in a frozen solution had been corroborated several years ago by complementary dynamic mechanical (DMA) and thermomechanical (TMA) analysis measurements of T. Schenz (6,12,13). Such a corroboratory approach has been recommended by Wolanczyk in another recent Letter to the Editor (11). Schenz used a computerized DuPont calorimeter with a time-averaged digital derivative feature to demonstrate that a sucrose solution, freeze-concentrated from an initial concentration of 20 weight % (w%) solute, exhibited a glass transition with the same characteristic value of T_g' at -32°C when measured (during warming at $5^\circ\text{C}/\text{min}$) by DSC, DMA, or TMA, as shown in Fig. 1 (6).

With regard to interpretation of low-temperature DSC thermograms (e.g. Fig. 3 in ref. 2) of frozen food materials, the schematic state diagram (modified from MacKenzie and Rasmussen, Fig. 18 (14)) in Fig. 2 (7) has been used to describe distinctive cooling/heating paths that can be followed by solutions of monomers (e.g. glucose) vs. oligomers or polymers (e.g. maltodextrin), starting from initial solute concentrations (C) less than that (C_g') in the freeze-concentrated glass at T_g' (3,15). In either general case, and regardless of initial cooling rate, rewarming from $T < T_g'$ forces the system through a solute-specific glass transition at T_g' , as explained in detail elsewhere (7). We have viewed Fig. 2 as a map whose topography reflects either two-dimensional energetics or three-dimensional kinetics, contingent on time-temperature-moisture dependence (16). The location of T_g' - C_g' represents a "universal crossroads", in that all paths of cooling/annealing/heating eventually lead to this site in a kinetic domain (7,16). T_g' - C_g' defines the kinetic conditions at the end of concomitant ice formation and freeze-concentration in real time on cooling to $T < T_g'$ (3,8,10), and conversely at the beginning of concomitant ice melting and melt-dilution of the solute in the aqueous rubber on heating to $T > T_g'$ (7). This description of the ice-melting process that begins at T_g' and ends at T_m (7) is entirely compatible with our consistent use (2-7,15-17) of T_m to signify the temperature at the END of crystal melting, in accord with the true thermodynamic definition of T_m and also the convention of polymer science (18,19). The shape of the equilibrium liquidus curve is defined energetically for very dilute solutions, based on colligative freezing point depression by solute (8). At concentrations of solute near or above the eutectic composition, melting of the metastable system is described by a non-equilibrium extension of the equilibrium liquidus curve (6,7,16). This is illustrated in the dynamics map shown in Fig. 3 (7), which is the actual equilibrium and non-equilibrium state diagram for sucrose-water. The shape of the non-equilibrium extension of the liquidus curve and its associated homogeneous nucleation curve (not shown) is kinetically determined by the underlying glass curve (6,7,16,41), as illustrated by the portion of the liquidus curve in Fig. 3 between the points T_e - C_e and T_g' - C_g' , where T_e is the eutectic

melting temperature (i.e. the T_m of pure crystalline ice plus pure crystalline solute) and C_e is the eutectic composition. T_g' is achieved by cryotechnologically useful solutes that do not readily undergo eutectic crystallization on cooling (e.g. sucrose). T_g' does not represent the incidental intersection of an independently existing equilibrium liquidus curve with the glass curve, but rather corresponds to the circumstantial intersection of the non-equilibrium extension of the liquidus curve and the underlying supersaturated glass curve that determined its shape (6,7,16).

We have stressed (7,16) that the time scale of mechanical relaxation processes (diffusion rates, deteriorative chemical reaction rates, structural stability, viscosity) of a system, including frozen food systems, is contingent on the location of the system on its dynamics map. Simatos et al. (1) also recognize the need to consider the state diagram before a relationship between the glass transition and stability of a frozen product can be explored. In this context, a cautionary note is appropriate, with respect to selection of the galactose-water system as a model and the experimental approaches used to construct the map for such a system (Fig. 1 in ref. 1). Definitions of the liquidus curve or M (at solute concentrations below the eutectic composition), glass curve or G , and T_g' are now in universal accord (1-10), in contrast to the mapped location of these thermal events. Construction of dynamics maps from calorimetric data requires an appreciation of critical aspects of the experimental approach and protocols for the appropriate use of thermal analysis techniques to investigate the equilibrium and non-equilibrium thermodynamic behavior of aqueous solutions as a function of solute concentration. The foundation for such an appreciation has been provided by Angell et al. (41) and Forsyth and MacFarlane (42). Their investigations of calorimetric behavior of aqueous solutions identified three kinetically-distinctive regions of concentration: solutions of (i) low solute concentration which undercool below their equilibrium liquidus curve, but from which ice eventually crystallizes during further cooling; (ii) intermediate concentration which vitrify without change in composition during rapid cooling, avoiding either nucleation or propagation before achieving the glassy solid state; but, devitrification and crystallization of ice occur during rewarming; (iii) high concentration which vitrify during normal cooling and from which ice does not readily crystallize during warming, due to the approach of the ice homogeneous nucleation curve to the glass curve (41); however, hydrates or solute may crystallize during cooling or rewarming. Accordingly, ambiguity is minimized during construction of a glass curve by selection of 1) a solute that avoids solute, eutectic, or hydrate crystallization; 2) an initial solute concentration in region (i) for characterization of aqueous glasses; and 3) diluent-free solute to characterize glasses with concentration greater than C_g' (2). Poly-

(vinyl pyrrolidone) and sucrose are justly popular as model solutes for glass systems (2,7). Selection of 20 wt solute as the standard initial concentration ensures reproducible freeze-concentration to the technologically-relevant composition at $T_g'-C_g'$ (2). In the particular case of the galactose-water system, and every other case in which solute or hydrate crystallization during cooling or rewarming cannot be ruled out explicitly, the transition under the melting peak (ΔQ) in DSC thermal profiles may not represent the enthalpy of melting (ΔH_m) of ice alone. Since the solutions used to construct the galactose-water state diagram (Fig. 1 of ref. 1) span the three kinetically-distinctive regions of initial concentration, the operative galactose concentrations responsible for the observed glass transitions would be incorrectly assigned because of previous crystallization of solute or hydrate, and therefore the glass curve could not be correctly constructed. In fact, it is evident that the glass curve in Fig. 1 of ref. 1 is incorrect, because it cannot be smoothly extrapolated to the T_g of water alone near -135°C (31). However, in order to construct a two-dimensional state diagram from data obtained using each of the three regions of initial concentration, pertinent cooling and heating rates would have to be used, corresponding to the critically different time scales of the relaxation behavior in the three concentration regions. Accordingly, the procedure recommended for the estimation of UFW content by extrapolation to zero of the measured total heat of melting of individual species after cooling and rewarming of solutions with a wide range of concentrations, spanning the three behavioral regions, is invalidated by this principle, regardless of whether the melting enthalpy of crystalline solute or hydrate can be deconvoluted from the overall ΔQ . Recognition of these aspects of the experimental approach and protocols used for the construction of dynamics maps urges caution in the superficial application of the method recommended by Simatos et al. (1), for estimation of the limiting UFW content and location of $T_g'-C_g'$ on the dynamics map.

The technological significance of T_g' to the storage stability of food systems, implicit in the description (7) of Fig. 2, has been the most important aspect of the thesis of our papers on cryostabilization technology (2). This assertion has been most convincingly validated (7) by the fact that T_g' of a freeze-concentrated solution, rather than T_g (site A in Fig. 2) of the original solution, is the ONLY glass transition temperature relevant to freeze storage stability at a given freezer temperature T_f , because almost all "frozen" products contain at least some ice. Consistent with XVQSUY in Fig. 2, the point of most relevance to the cooling/warming rates practiced in industry is the point at which commercial freezing processes induce ice formation beginning at point Q on the dynamics map, where homogeneous nucleation after some extent of undercooling. Since the temperature

point Q is generally near -20°C (20) and well above that at point A, this lower T_g of the glass with the original concentration of solute(s) typical of a high-moisture product is never attained and has no practical consequence (7). Once ice formation and freeze-concentration occur in a frozen product, the material-specific T_g' of the salient freeze-concentrated matrix becomes the one and only glass transition temperature that controls product behavior during storage at any freezer T_f below T_m and either above or below T_g' (7). Of course, multiple localized amorphous domains of freeze-concentrated solute(s)/UFW can coexist in frozen foods, particularly natural products, which consist of spatially inhomogeneously-distributed and/or thermodynamically incompatible mixtures of water-compatible materials, and the multiple respective values of T_g' can be observed and have been measured by DSC (6,7).

Simatos et al. (1) focus most of their discussion on our advocacy (2-7,15-17, 21,25,26) of WLF kinetics (22) to describe rates of diffusion-limited relaxation processes (e.g. deteriorative changes during storage) in amorphous or partially crystalline, water-containing food systems in the rubbery temperature range between T_g and T_m (highlighted in the schematic dynamics map in Fig. 4 (6)). They point out (1) that our conceptual application of the WLF equation as a theoretical tool to analyze and predict storage stability (4,15,21) of low-moisture ($C > C_g'$) food systems represents a "very interesting approach". Of course, it should be recalled that "for a generation of [synthetic] polymer scientists and rheologists, the WLF equation has provided a mainstay both in utility and theory" (23). We thank Simatos et al. (1) for commending "as a very positive contribution [our] underlining of the WLF behavior of viscosity in rubbery materials to explain the influence of temperature on the stability of frozen products". We have pointed out previously (7), as Simatos et al. do also (1), that extension of the applicability of WLF kinetics to high-moisture ($C < C_g'$) frozen food systems, while expected to be valid on theoretical grounds, is still an open question that warrants further experimental investigation and verification. An area of particular interest concerns the influence of temperature on diffusion-limited reactions (24), both in the subzero temperature range between T_g' and the T_m of ice (as highlighted in Fig. 4) for frozen products and within the higher T_g - T_m range relevant to low-moisture products. These kinetically-metastable domains above the glass curve define the regions where WLF behavior is expected, and their location on the dynamics map remains unchanged, even though solute or eutectic crystallization is avoided (as frequently is the case with food solutes which are useful for cryotechnology). However, this issue of the extent of applicability of WLF kinetics is separate from the other issue, the "feasibility of the practical determination of T_g for food materials", raised as a related and also still open question by Simatos et al. (1).

In the last few years, there have been numerous publications of T_g for many different low-moisture food materials, systems, and products (and references therein), as well as recent publications of T_g' values for a wide variety of real, complex frozen food materials and products. These follow-up studies representing continued progress beyond earlier studies of simple model systems (2-5,16). In light of this body of work by internationally recognized food scientists, we suggest that the "feasible practical determination of T_g for food materials" has already been demonstrated.

Simatos et al. (1) protest our aggrandizement of the salience of T_g and of the contrast between WLF kinetics and Arrhenius kinetics in the time-temperature-moisture dependence of mechanical relaxation in food systems. WLF kinetics differ from Arrhenius kinetics in several respects (6,16), and we continue to emphasize the contrast because that the qualitative differences are as influential as the quantitative differences in their impact on both experimental approach and technological practice. A comparison between WLF and Arrhenius kinetics begins with the realization that the temperature dependence of microscopic relaxation processes, including the self-diffusion coefficient, viscosity, rotational and translational relaxation rates or times; and macroscopic processes that rely on diffusion, monotonically from a steep dependence of log relaxation rate on temperature just above T_g to a shallow dependence above T_m ; i.e. over a material-specific temperature range from T_g to far above T_g (16). This realization has underlying diagnostic characteristics that distinguish WLF from Arrhenius kinetics. First, the coefficient of the temperature dependence (the activation energy) is defined as a constant in the expression for Arrhenius kinetics, and a plot of log relaxation rate vs. $1/T$ is a straight line; the coefficient itself is temperature dependent in the WLF expression. Second, log relaxation rate vs. $1/T$ is characteristically curvilinear in a specific temperature range between T_g and T_m , approaching linearity above T_m and far above T_g (6). The absolute value of the derivative of log relaxation rate vs. $1/T$ increases as T_g is approached from above, and approaches an approximately constant value as the temperature falls above T_m and far above T_g , where the constant value corresponds to the activation coefficient (activation energy) which characterizes the particular relaxation process. The shape of the derivative profile and the temperature range over which the derivative varies are material-specific. Typically a range of $\geq 100^\circ\text{C}$ for materials with a ratio of T_m/T_g of > 1.5 and of $< 100^\circ\text{C}$ for materials with a ratio of $T_m/T_g < 1.5$ (16). Cl

fact that the derivative varies in a material-specific and temperature-dependent fashion, rather than the particular magnitude of the derivative, that constitutes the salient feature of WLF kinetics. Second, there is no explicit reference temperature in the expression for Arrhenius kinetics, because, in fact, the implicit reference temperature is taken generically to be 0 K, regardless of the distinctive thermomechanical properties of a system, and even though Arrhenius kinetics are applicable only below T_g and above T_m (8,15,22). In contrast, the WLF expression benefits from an explicit material-specific reference temperature, which is the T_g of a component or compatible blend (22). Therefore, it is critical to note that when the rate or time scale of a relaxation process can be shown to depend on a material-specific reference T_g , Arrhenius kinetics are not applicable to describe mobility transformations (time-temperature-moisture superpositions) for that process in the rubbery range from T_g to T_m , regardless of whether the average slope of the $\log k$ vs. $1/T$ curve can be empirically fitted by a $Q_{10} = n$ rule and regardless of the particular magnitude of n . In summary, in the temperature and composition domain sufficiently above T_g , where equilibrium and steady-state thermodynamics apply, the coefficient of the temperature dependence of \log relaxation rate is defined by Arrhenius kinetics to be a constant and is observed to approximate a relatively small constant value over a typical experimental range of about 20°C (37). In the increasingly non-equilibrium domain of temperature and composition approaching T_g from above, the coefficient of the temperature dependence of \log relaxation rate on $1/T$ is not a constant and increases evermore rapidly over a range of 20°C (16). Typically, Arrhenius rates for aqueous systems above T_m might increase four-fold over a temperature range of 20°C (37), while WLF rates near T_g would increase by 4 or 5 orders of magnitude (6,10,16). As an example illustrating the significance of the difference between WLF and Arrhenius kinetics, Chan et al. (27) have noted that the dielectric relaxation behavior of amorphous glucose plasticized by water is "remarkably similar" to that of synthetic amorphous polymers in glassy and rubbery states. They showed that the rates of this mechanical relaxation process, which depends on rotational rather than translational mobility, follow the WLF equation for water-plasticized glucose mixtures in their rubbery state above T_g , but follow the Arrhenius equation for glucose-water glasses below T_g (27). Also noteworthy is Angell's (39) pertinent observation that the temperature dependence of the transport and relaxation properties of undercooled liquid water is strikingly non-Arrhenius in the temperature range from T_m to the homogeneous nucleation temperature at -40°C (corresponding to a portion of the WLF rubbery domain shown in Fig. 4). This non-Arrhenius temperature dependence also typifies the case for many other viscous liquid systems which undergo restructuring processes that require the "cooperative in-

volvement of other molecular motions" (39). Included in these other viscous liquid systems that exhibit non-Arrhenius behavior are concentrated aqueous solutions at subzero temperatures, according to a suggestion by Hofer et al. (1).

On the other hand, Simatos et al. (1) believe that the contrast between kinetics and Arrhenius kinetics is less important than "that the apparent activation energies of viscosity change in the vicinity of T_g are much higher than the 'activation energies' for viscosity or diffusion in liquids." We prefer the principle to discourage the calculation and use of apparent activation energies in discussion of systems located in the kinetically-metastable domains of the dynamics map, where the instantaneous or operational value of an activation energy is both time-dependent and temperature-sensitive (6,7). Moreover, partial values of activation energy lend little insight to comparative time scale relaxation processes. Simatos et al. (1) refer to a hypothetical case with T_g of -30°C and WLF coefficients (unstated) of 17.44 and 51.6 (Fig. 2 of ref. 1) for which activation energies near T_g , 20°C above T_g , and 50°C above T_g are approximated as 370, 230, and 140 kJ/mole, respectively. We can also refer to actual systems for which those values of the WLF coefficients have been determined: glucose (22) and sucrose-fructose-water blends (32). For diluent-free glucose, with T_g of 31°C (16), analogous activation energies near T_g , 20°C above T_g , and 50°C above T_g are 575, 355, and 205 kJ/mole. For a 83:12:5 by weight of sucrose:fructose:water with T_g of 40°C (32), analogous activation energies are 610, 375, and 220 kJ/mole. In all three cases, the time scale of microscopic viscosity would change equivalently by 4 or 5 orders of magnitude in the 20°C interval above T_g (6,10,16), but the activation energies change equivalently and uninformatively for the three cases. The inherent benefit of the WLF expression as a superpositioning tool (22) is that it provides a qualitative and predictive understanding of time-temperature-moisture transfer processes which are scaled according to ΔT or ΔC for each system relative to its glass transition curve. Recognition of the T_g' - C_g' glass as the manifestation of a kinetic barrier to any diffusion-limited process (2,3,10), including further ice nucleation on cooling (within an experimental time frame), despite the continued presence of UFW at all temperatures below T_g' , is conceptually more satisfying than the postulation of an energetic barrier, in the form of a "high activation energy kinetic barrier to relaxation processes has been identified as the extreme temperature dependence (defined by a WLF expression) that governs changes in local viscosity and free volume (and consequently, heat capacity) just below T_g' (6,7). This perspective on the glass at T_g' - C_g' as a mechanical barrier to operatively-constrained mobility and diffusion has provided a long-sought theoretical explanation of how undercooled water can persist (over a real time period) in a solution in the presence of ice crystals (6,7).

With regard to the applicability of WLF kinetics to rubbery, ice-containing systems, Simatos et al. (1) claim that we have oversimplified the description of the situation in a frozen product at $T_g' < T < T_m$ of ice, and they "are surprised that [we] never discuss" the different temperature-dependent phenomena, such as the effect of melt-dilution of an amorphous solute/UFW mixture at $T > T_g'$ on its viscosity and chemical reaction rates. Again, we are surprised by this sweeping criticism. While our earlier Cryo-Letters article (2) was admittedly a long review, it was nevertheless of finite length and could not be (nor was it invited to be) all-inclusive in scope. Moreover, the topic of melt-dilution/freezing-concentration had already been elegantly and extensively described by Franks (43), who gave examples of in vitro and food/biological systems to illustrate the magnitudes and pertinent temperature ranges of relative contributions of melt-dilution vs. temperature change on viscosity and chemical reaction rates in the temperature region between T_g' and T_m . The contribution of melt-dilution predominates over the contribution of change in temperature in the upper temperature range of the equilibrium or near-equilibrium liquidus above the eutectic melting temperature. Below T_e , the effect of temperature begins to dominate over the effect of melt-dilution and becomes increasingly predominant in the lower temperature range of the non-equilibrium liquidus approaching T_g' . The magnitude of the contribution of melt-dilution depends strongly on the initial solute or reactant concentration before freezing. In the case of the effects of melt-dilution on the kinetics of the acid-catalyzed mutarotation of glucose (Fig. 3.14 of ref. 43), taken as a model for such effects (43), melt-dilution causes about a six-fold decrease in rate far above T_g' , when the initial concentration of glucose before freezing is about 1 wt. At high initial glucose concentrations, rate diminution due to melt-dilution is not pronounced (43); melt-dilution causes about a two-fold decrease in rate when the initial glucose concentration is about 10 wt. In contrast, the total change in diffusion rates in the temperature range between T_g' and T_m would exceed 10 orders of magnitude for any initial glucose concentration less than C_g' (6,32,43). In consideration of the previous literature and the lesser dominance of melt-dilution effects on kinetics in the temperature region between T_g' and T_m , we emphasized the direct effects of temperature in the Cryo-Letters review (2). However, we have discussed the effect of melt-dilution on viscosity for the interesting case of sucrose-water mixtures in the rubbery temperature range between T_g' and the T_m of ice, as excerpted below from a subsequent paper (7).

The dynamics map for sucrose-water in Fig. 3 has provided several noteworthy revelations concerning the relative locations of the glass, solidus, and liquidus curves (7). Just as the liquidus curve describes the melting of crystalline solvent, in this case ice, the solidus curve describes the melting of crystal-

line solute. The melting process is called dilution when crystalline solvent melts in the presence of solution or dissolution when crystalline solute melts in the presence of its saturated solution. The solidus curve for the melting of crystalline sucrose decreases from $T_m = 192^\circ\text{C}$ for dry sucrose (16,21), through several points for saturated sucrose solutions at different temperatures (28), to $T_e = -14^\circ\text{C}$ at $C_e = 62.3$ wt sucrose (29). The glass curve decreases from $T_g = 52^\circ\text{C}$ for dry amorphous sucrose (16,20,21,30), through $T_g' = -32^\circ\text{C}$ at $C_g' = 64$ wt sucrose (4,12,20,30), to $T_g = -135^\circ\text{C}$ for pure amorphous solid water (31). The point T_e - C_e is located at the intersection of the equilibrium solidus and equilibrium liquidus curves, while the point T_g' - C_g' is located at the intersection of the non-equilibrium liquidus and glass curves. As illustrated by the schematic state diagram in Fig. 4, the temperature interval $\Delta T = T_e - T_g'$ between T_e (as a particular value of T_m of ice) and T_g' would correspond to an atypically small WLF rubbery domain of only 18°C (relative to the typical $T_m - T_g$ range of about 100°C for many diluent-free, synthetic amorphous polymers (6, 16,22)), over which the microscopic viscosity (η) of the sucrose-water solution would be estimated to decrease by about 13 orders of magnitude from the characteristic η (η_g) at T_g' (16,22,32). [This value of $\Delta\eta$ was estimated as follows (7): a) at T_g' - C_g' , $\eta_g \approx 10^{13}$ Pa s (32), b) at 20°C , $\eta \approx 0.1$ Pa s for 62.3 wt sucrose (28), and c) at T_e - C_e , $\eta_e \approx 1$ Pa s, based on an assumption of Arrhenius behavior between -14 and 20°C (i.e. at $T > T_m$, $Q_{10} = 2 \rightarrow$ a factor of 10 change for a ΔT of 33°C) (16).] Consequently, the rates of deteriorative changes that depend on constrained diffusion in a frozen aqueous system of pure sucrose would be predicted correspondingly to increase by about 13 orders of magnitude vs. the rates at T_g' (7), with profound implications for the storage stability and kinetics of "collapse" processes in frozen food systems (e.g. ice cream and other frozen desserts and novelties) for which a freeze-concentrated sucrose solution could serve as a limiting model (2-6). It has been noted (7) that the 13 orders of magnitude predicted from the WLF equation for the decrease in microscopic viscosity and concomitant increase in diffusion-limited relaxation rate over a rubbery domain with a temperature span from T_g' to $T_g' + 18^\circ\text{C}$ are based only on the effect of increasing temperature above the T_g' reference state, and not on any effect of dilution due to the melting of ice, which would begin on heating to $T > T_g'$, on the solute concentration in the rubbery fluid. Such an effect of melt-dilution would obviously cause a further decrease in viscosity over-and-above the WLF-governed behavior (1,7). The resultant effect on diffusion-limited reaction rate (e.g. of enzyme-substrate interactions (3)) would not be so obvious (1,7). The rate could increase or decrease (1,7), depending on whether or not the solute being diluted is a participant in the reaction (33). The sucrose-water system shown in Fig. 3 is re-

markable with respect to the minimal effect of melt-dilution on heating from T_g' to T_e (7). The sucrose concentration only decreases by 1.7 wt%, from $C_g' = 64$ wt% to $C_e = 62.3$ wt%, over a temperature range of 18°C , due to the near-vertical path (compared to the path of colligative freezing point depression in the equilibrium portion) of the extremely non-equilibrium extension of the liquidus curve at $C > C_e$ (7). Despite this fact, the above discussion is not meant to negate the importance of melt-dilution (stressed by Simatos et al. (1)) as temperature is increased above T_g' . Analogous to experience in drier systems at $T > T_g'$ and $C > C_g'$ (21), either addition of water (corresponding to a ΔC) or increase in temperature (ΔT) above the glass curve accomplishes decreased relaxation times (15,16). However, water-rich systems differ from drier systems in that water is equivalently as effective as temperature as a plasticizer for drier systems at $C > C_g'$, but the practical limit of efficacy of water as a plasticizer is exceeded at $C < C_g'$ (16,26).

As noted by Simatos et al. (1), we have reported limited experimental results for storage stability of ice creams and other frozen novelties (originally in (2) and, after refinements, in (6,7)). As shown in Fig. 5 (6,7), these results have been interpreted as a demonstration that the rate of ice crystal growth during freezer storage increases with increasing T_f as ΔT above T_g' , in a manner predicted by WLF, rather than Arrhenius kinetics. Here, and consistently in the past (2,6,7), we have followed the convention of the life sciences that an unqualified reference to Arrhenius kinetics implies temperature dependence with $Q_{10} \approx 2$ (37,44). (In contrast, Simatos et al. (Fig. 2 of ref. 1) use Q_{10} without qualification to refer to $Q_{10} = 10$ as an analogy to Arrhenius kinetics.) As illustrated in Fig. 5B, the extent of ice crystal growth after a fixed storage time, chosen to insure that ice crystal size had not yet reached a limiting value, increased more dramatically with increasing ΔT than predicted by a typical $Q_{10} = 2$ rule of Arrhenius kinetics (dashed line in Fig. 5B). As previously explained elsewhere (6,7), the experimental data in Fig. 5 had originally been plotted as straight lines (Fig. 15 in ref. 2), in part for simplicity of presentation, and in part because the numerical coefficients C_1 and C_2 in the appropriate WLF equation (22) are unknown and cannot be assumed for such frozen products. We have subsequently compared the qualitative curvature of the data plots in Fig. 5 to a plot of the WLF equation with its "universal" numerical values of C_1 and C_2 (22), shown in Fig. 6 (6,7) (and also as curve 1 in Fig. 2 of ref. 1). This closer approximation of the data in Fig. 5 by WLF, rather than Arrhenius $Q_{10} = 2$, temperature dependence has been viewed (6,7) as support for the earlier conclusion (2) of the applicability of WLF kinetics to such rubbery frozen foods as ice cream. Equally as important, the existence of material-specific reference temperatures, identified as the values of T_g' dictated by the

particular formulations of the products and dictating in turn the T_f below which no ice crystal growth was detectable during the storage test, confirmed the conclusion of the applicability of a WLF interpretation. [Although Simatos et al. (1) are certainly entitled to express reservations about the quantitative nature of our published data on ice crystal growth rates in ice creams and other frozen novelties and to question our "rigorousness of reasoning" regarding those data, we feel compelled to defend the Ph.D. psychosensory physiologist who trained the sensory panelists. The technological importance and practical relevance of the meticulous and reproducible results of such industrial sensory panels are demeaned by naively referring to their contributions as "folklore" and not "true experimental investigation" (1).]

We commend Simatos et al. (1) for their attempt to use selected experimental data from the literature to assess the importance of WLF behavior to the stability of frozen food products, since these products exist as rubbery fluid matrices surrounding included ice crystals at freezer temperatures above the relevant, product-specific values of T_g' . However, their analyses of data for various systems at subzero temperatures were based on T_g values of questionable validity. Some of these T_g values were said to be measured, others estimated or deduced (1). This issue is critical to a conclusive and unambiguous evaluation of the importance of WLF behavior to the stability of frozen foods, because the selection of a correct T_g value is in fact the basis for a definitive analysis of WLF kinetics (22). As explained previously, T_g' is the only location on a system-specific glass curve that corresponds appropriately to the subzero reference state for WLF behavior of an ice-containing, rubbery fluid system (7, 15). Thus, T_g' represents the temperature boundary below which Arrhenius kinetics would be expected to apply to an ice-containing, glassy solid matrix of a frozen product (15,16). Selection of an incorrect T_g' value for the reference state of a frozen product would eliminate the ability to predict the subzero temperature ranges appropriate to the expected observation of WLF or Arrhenius kinetics. For example, if the actual value of T_g' for a frozen product were -10°C , but an incorrect value of -40°C were assumed for data analysis, then one would incorrectly expect to see WLF behavior in the temperature range from -40 to -10°C , whereas Arrhenius behavior should actually have been predicted in this range. As a consequence, one might conclude prematurely, from the absence of WLF behavior in this temperature range, that WLF behavior was unimportant to the stability of such a frozen product.

A pioneering study by Soesanto and Williams (32) had previously shown that the high viscosities of concentrated solutions (92-98 wt solids) of water-plasticized, non-crystallizing sugar blends of sucrose and fructose (7:1 w:w) at $2 < T < 80^\circ\text{C}$, plotted as $\log(\eta/\eta_g)$ vs. $(T - T_g)$ for temperatures from 20 to 9

C above T_g (i.e. within the rubbery range), fit very well the master curve of the WLF equation with its "universal constants". The success of this technologically-important and theoretically-enchaining demonstration owed to a) the valid selection of T_g values for the experimental aqueous sugar blends, and b) the use of combinations of sugar concentrations and experimental temperatures always well within the WLF region between the solidus and glass curves (32). Simatos et al. (1) have attempted similarly to compare WLF behavior to the influence of temperature in the range -30 to 0°C on the viscosity of a 75% sucrose solution containing no UFW, as illustrated by a superposition of the WLF expression on a plot of $\log \eta$ vs. T for the experimental data in curve (a) of their Fig. 3 (1). However, Simatos et al. (1) mention (without explanation) that the $T_g = -64^\circ\text{C}$ deduced from their representation is "somewhat lower" than their T_g value measured by DSC. This is not surprising, since the value of T_g for a 75 wt% sucrose solution is -8°C , as interpolated from the sucrose-water glass curve (our Fig. 3) constructed from measured values of T_g (7,20,30). As a result, viscosity results for 75 wt% sucrose in the temperature interval from -8 to -30°C are expected to show Arrhenius kinetics, though not necessarily of the $Q_{10} = 2$ form. In fact, the temperature range corresponding to most of the solid curve (a) of their Fig. 3 (1) falls below T_g and represents the region below the WLF domain, rather than the upper region of the WLF domain as presumed in their Fig. 3. Thus, as should have been expected, the data of curve (a) do not complement the results of Soesanto and Williams (32), and WLF behavior was not observed. In contrast, in their Fig. 3 curve (b), Simatos et al. (1) show calculated data for freeze-concentrated sucrose solutions in the temperature range from -30 to -10°C , such that the experimental temperature interval was always within the WLF domain between T_g' at -32°C and T_m of ice in sucrose solution only slightly more dilute than the eutectic composition (7). Because the magnitude of this WLF domain is very much smaller than 100°C , the coefficients of the appropriate WLF expression are quite different from the "universal" values (16). In fact, the change in $\log \eta$ vs. T shown in curve (b) is exactly what would be expected for WLF behavior when the temperature interval between T_g and T_m is small, similar to the case shown in Fig. 4c of ref. 16. The minor extent of dilution in the temperature interval between -30 and -10°C would not contribute significantly to the temperature dependence of viscosity, as previously explained. Despite the fact that the CHANGES in $\log \eta$ vs. T are entirely as expected -- Arrhenius (but not $Q_{10} = 2$) behavior below T_g for curve (a) and WLF (but not "universal" coefficients) behavior between T_g' and T_m for curve (b) -- there are two puzzling features of Fig. 3 of Simatos et al. (1). We wonder what is meant by "equilibrium concentrations" (1) of freeze-concentrated sucrose solutions, since such supersaturated, undercooled, unstable sucrose-water rub-

bers are by definition non-equilibrium systems. Although ~~no un-~~ are indicated (1), cP is inferred from the superimposed ~~WLF ma-~~ the viscosity scale is meant to be the same for curves (a) and difficult to imagine how freeze-concentration could produce a sol viscosity than that of 75 w% sucrose, in which no ice ~~can occu~~

Simatos et al. (1) have analyzed data from the literature co bility of soluble protein in frozen cod and ascorbic ~~acid in f~~ storage temperatures ranging from about -30 to -15°C ~~and from~~ spectively. For both of these ice-containing products, ~~they h~~ mon T_g (presumably they mean T_g') of -40°C "as an approxiimate sideration of thermograms of beef muscle, etc. (adopting the l definition of T_g , although our interpretation of these ~~thermo~~ to a much lower figure)" (1). It is curious that "adopting [o T_g " could have led to such an assumption, and we ques~~tion~~ the as a reasonable approximation of the predominant T_g' ~~value th~~ the overall storage stability of frozen cod, peas, ~~and~~ beef ~~m~~ determine the type of kinetics operative during storage at a

We have measured the predominant T_g' values for the ~~following~~ fish, and vegetable products (6,7,25,26): beef and ~~chicken~~ -13.5°C ; pork loin -20°C ; tuna fish -11.5 to -18°C ; peas -25.5°C ; green beans -27.5°C ; broccoli -26.5°C ; ~~cauliflow~~ ach -17°C ; potato -11 to -16°C ; and sweet corn -8 to $-$ cited for tuna, potato, and corn correspond to T_g' ~~values me~~ different samples and/or different locations within ~~individu~~ have also measured T_g' values for a number of high ~~molecular~~ teins, which may serve as models for the major prote~~in~~ in compe beef muscle, e.g. collagen, gelatin, bovine serum ~~albumin~~, e ues range from -5 to -16°C (6,25). Our measured T_g' ~~of~~ -25°C lar to the T_g' values for several other vegetables. ~~In all~~ of a given vegetable is determined by, and diagnostic of, its solids composition (7), predominantly in terms of ~~the~~ ~~weigh~~ (starch, other polysaccharides, proteins) to small ~~metaboli~~ acids). Results of studies of enzymatic activity ~~during~~ sto beans (34), frozen parsley (35), and frozen cauliflower (38 to the validity and technological significance of ~~the~~ T_g' value these and other vegetables with comparable sacchar~~ide~~ ~~polym~~ solids compositions, including peas. For example, ~~Lee~~ et al reported quality changes due to significant residual ~~enzym~~ after blanching) in frozen green beans, during storage at T_g'). Baardseth and Naesset (38) have reported ana~~logous~~ fi

cauliflower. They found that "unblanched cauliflower was inedible and sensorially unacceptable after 4 weeks' storage at -20°C " (38) (i.e. $T_f > T_g'$), due to the activities of lipid-degrading enzymes. Duden and Scholz (35) have shown that the extent of enzymatic degradation of lipids and concomitant quality loss during frozen storage of parsley increase dramatically with increasing T_f . Sensory quality deteriorates noticeably after only 2 months at -18°C but changes negligibly after 1 year at -24°C , while the decomposition reactions cease at $T_f < -32^{\circ}\text{C}$. Such behavior would be predictable for a product with a T_g' of about -25°C . From our measured T_g' values for tuna, meats, and proteins, we would choose -15°C as a reasonable approximation of T_g' for frozen cod. This choice is supported by results of a recent study of storage stability of frozen cod by LeBlanc et al. (36), who have noted that enzymatic reaction rates and corresponding rates of quality loss increase with increasing T_f , most dramatically at storage temperatures of -5 to -10°C (i.e. $T_f > T_g'$). Thus, we favor approximate T_g' values of -25°C for frozen peas and -15°C for frozen cod, rather than the common value of -40°C assumed by Simatos et al. (1).

This significant discrepancy in the selection of T_g' values appropriate to an analysis of the kinetics of deteriorative changes in frozen cod and peas suggests alternatives to the interpretations by Simatos et al. of the results shown in Fig. 4 of (1). They state that "the straight lines of Fig. 4 (1) are not characteristic of WLF kinetics, but on the contrary are consistent with the definition of Q_{10} " and attribute the observed temperature dependence of the deterioration processes to the dilution effect of ice-melting (1). For frozen peas with $T_g' = -25^{\circ}\text{C}$ and a small WLF domain characteristic of freeze-concentrated systems, stability data for loss of ascorbic acid would be expected to reflect WLF kinetics with steeper temperature dependence than the "universal" WLF expression at storage temperatures just above T_g' (16). At higher storage temperatures, always within the metastable range from T_g' to T_m , in the reported experimental range from -18 to -1°C , complex kinetics are expected, ranging from WLF behavior at the lowest experimental temperature to behavior modified by melt-dilution at the higher experimental temperatures (43). The complexity is increased by the contribution of free radicals to the mechanism of loss of ascorbic acid (43). Close inspection of curve (b) of their Fig. 4 (1) suggests a diminution of rates at the highest storage temperatures (which may reflect the effect of melt-dilution (43)), rather than a straight line for the temperature dependence. If curve (b) of their Fig. 4 were shifted by 15°C to the left along the abscissa (i.e. $T_g' = -25$ rather than -40°C) and compared to a WLF expression with the appropriate non-universal coefficients such that the curve is steeper at T_g and shallower above T_g (16), there would be much less difference between the WLF curve and the straight line of slope corresponding to $Q_{10} =$

17.8. The interpretation of the results shown in Fig. 4 curve (a) (1) for residual solubility of proteins of frozen cod stored at T_f about -30°C is also more ambiguous than suggested by Simatos et al. (1). As mentioned earlier, for a product with $T_g' = -15^\circ\text{C}$, stability data for storage at temperatures below this T_g' would be expected to follow Arrhenius kinetics (but not necessarily with $Q_{10} = 2$), rather than WLF kinetics (8,15,16). This appears to be the case for the data in Fig. 4 curve (a) of (1), which is similar to the data for storage at $T_f = -10^\circ\text{C}$ under causative conditions and resulting value of $Q_{10} \approx 10$ to curve (a) of (1) for 75 w% sucrose solution. However, the recent report of LeBlanc et al. (36) is in apparent contrast to these results presented by Simatos et al. (1). The results of LeBlanc et al. (36) for frozen cod fillets stored at -15°C , and -12°C show that the dependence of enzymatic reaction rates on temperature cannot be predicted by an Arrhenius expression, as evidenced by non-linearity of $\log k$ vs. $1/T$, primarily due to the data corresponding to $T_f = -12^\circ\text{C}$ mentioned earlier, such non-linear Arrhenius plots can be diagnostic of a phase transition in the fish muscle (6). LeBlanc et al. have suggested that their non-linear Arrhenius behavior (6). LeBlanc et al. have suggested that their non-linear Arrhenius behavior "could be due to a real phenomenon where the activation energy changes at a phase transition in the fish muscle" (36). We suggest that the "transition" mentioned by LeBlanc et al. (36) is the glass transition of the freeze-concentrated, protein-rich matrix, with a predictable T_g' of -15°C (6,7). Recognition that this T_g' value would demarcate the rubbery region of WLF kinetics at higher storage temperatures (e.g. -12°C) from the solid region of Arrhenius kinetics at $T_f < T_g'$ provides an explanation for the conciliation of the conflicting results of Simatos et al. (1) and LeBlanc et al. (36). An additional note of caution relates to the interpretation of storage stability with respect to protein solubility and enzymatic reaction rates. Protein denaturation leading to insolubilization and loss of enzymatic activity can be caused by low temperature per se or concentration and irreversible aggregation due to freeze-dehydration or both (43,44). Careful analysis is required that immediate freeze-thaw damage be distinguished from longer-term storage deterioration, since both of these contributions depend on storage time, storage/thawing rates and freezer temperature (6,43,44).

Simatos et al. (1) have also analyzed literature data for storage stability of egg yolk. For their plot (Fig. 5 of ref. 1) according to the WLF equation, they used a T_g value of -39°C , once again with the curious attribution for the determination of T_g' , which they have evidently misinterpreted (2,3). As mentioned earlier, we have measured T_g' values ranging from -15.5°C for many high MW proteins, including several different albumins (6,25) to -15.5°C and egg globulins ($T_g' = -10.5^\circ\text{C}$) (6,25). While we have

ed the T_g' of egg yolk per se, the water-compatible solids in egg yolk include high MW proteins comparable to many we have measured, and we favor a value of about -10°C , rather than -39°C (1), as a reasonable approximation of the T_g' for egg yolk. In this context (as for frozen cod), it is not at all surprising when Simatos et al. report that "in the temperature range between -39 and -11°C , an Arrhenius behavior is rather satisfactorily obeyed" (1), because it is precisely the behavior that should be expected in the glassy solid state at $T_f < T_g'$ for a product with a T_g' of -10°C . Therefore, the results of this analysis by Simatos et al. (1) do not represent an invalidation of WLF behavior, as these authors seem to imply. Obviously, such Arrhenius behavior would have nothing to do with any effect of melt-dilution (as Simatos et al. suggest (1)), because ice-melting would not begin until T_f exceeds T_g' . Indeed, the effect of dilution above our suggested value of T_g' at -10°C is quite apparent by the change in slope in Fig. 5 of (1).

Simatos et al. argue that "Levine and Slade are wrong in presenting their approach as an all-embracing one" (1). If that had been our intention, we would deserve to be criticized for it. However, our actual goal has been well-stated by Simatos et al. themselves (1), to "draw the attention of food scientists to concepts which were first developed in the field of polymer chemistry." In our previous papers on the "food polymer science" approach to cryostabilization technology (2-7), we have emphasized the potential importance of a) glass transitions in food products and processes, b) dynamics maps including equilibrium and non-equilibrium aspects of state diagrams of food systems, c) water as a plasticizer of amorphous food materials, d) WLF kinetics in rubbery food systems, and e) T_g' to the quality and storage stability of ice-containing frozen products; in an attempt to f) present, as a new alternative, a tried-and-tested approach that has become well-established and widely accepted in another technical discipline (i.e. synthetic polymer science), g) document illustrations of the applicability and utility of this approach, and of the insights and advances in qualitative understanding gained from this new perspective on food products and processes, and h) interest other food scientists and technologists (including leaders in the field, like Simatos et al.) in considering, testing, and exploring the scope of this approach and its usefulness to the study of foods.

Simatos et al. (1) ended on a positive and constructive note, concluding that "it appears that an important part may certainly be played in the kinetics of physical, chemical, and biochemical processes taking place in frozen products by the decrease in viscosity of the CAS according to WLF behavior" and that further experimental investigations are needed in this area. We could not agree more with the entire statement, and have in fact said much the same thing in

our most recent follow-up paper (7) to our earlier Cryo-Letters review (2). We are sure Simatos and coworkers would agree with our opinion that a critical part of future investigations in this area will be the accurate characterization of T_g' values by corroborative combinations of DSC, DMA, TMA, and other techniques suited to the frozen systems to be studied.

ACKNOWLEDGMENTS

We thank Simatos, Blond, and Le Meste for sharing an earlier version of their Letter with us, and especially for the opportunity and challenge to engage in such stimulating and constructive personal correspondence and scientific dialogue on an important issue in the field of food cryotechnology. We also thank the Editor of this Journal for allowing and encouraging such beneficial exchanges of scientific viewpoints.

REFERENCES

1. D. Simatos, G. Blond and M. Le Meste. *Cryo-Lett.* 10, 77-84 (1989).
2. H. Levine and L. Slade. *Cryo-Lett.* 9, 21-63 (1988).
3. H. Levine and L. Slade. *Carbohydr. Polym.* 6, 213-244 (1986).
4. H. Levine and L. Slade, in *Food Structure - Its Creation and Evaluation*, ed. J.R. Mitchell and J.M.V. Blanshard, Butterworths, London, 1988, pp. 149-180.
5. H. Levine and L. Slade. *J. Chem. Soc., Faraday Trans. I* 84, 2619-33 (1988).
6. H. Levine and L. Slade, in *Thermal Analysis of Foods*, ed. C.-Y. Ma and V. Harwalkar, Elsevier Applied Science, London, 1989, in press.
7. H. Levine and L. Slade. *Comments Agric. Food Chem.* 1, 315-396 (1989).
8. F. Franks, in *Water: A Comprehensive Treatise*, ed. F. Franks, Vol. 7, Plenum Press, New York, 1982, pp. 215-338.
9. F. Franks, M.H. Asquith, C.C. Hammond, H.B. Skaer and P. Echlin. *J. Microsc.* 110, 223-238 (1977).
10. F. Franks, in *Properties of Water in Foods*, ed. D. Simatos and J.L. Mulder, Martinus Nijhoff, Dordrecht, 1985, pp. 497-509.
11. J.P. Wolanczyk. *Cryo-Lett.* 10, 73-76 (1989).
12. T.W. Schenz, M.A. Rosolen, H. Levine and L. Slade, in *Proceedings 13th NATAS Conference*, ed. A.R. McGhie, Philadelphia, 1984, pp. 57-62.
13. T.W. Schenz, at 24th Soc. Cryobiology Meet., Edmonton, Alberta, June 2, 1987.
14. A.P. MacKenzie and D.H. Rasmussen, in *Water Structure at the Water-Polym. Interface*, ed. H.H.G. Jellinek, Plenum Press, New York, 1972, pp. 146-

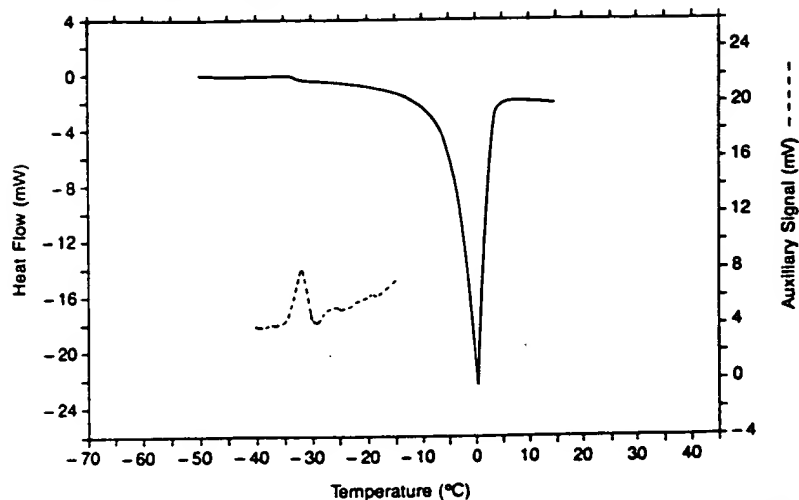
15. H. Levine and L. Slade, in *Water Science Reviews*, ed. F. Franks, Vol. 3, Cambridge University Press, Cambridge, 1988, pp. 79-185.
16. L. Slade and H. Levine. *Pure Appl. Chem.* 60, 1841-1864 (1988).
17. L. Slade and H. Levine. *Carbohydr. Polym.* 8, 183-208 (1988).
18. P.J. Flory, *Principles of Polymer Chemistry*, Cornell University Press, Ithaca, 1953.
19. B. Wunderlich, *Macromolecular Physics*, Vol. 3 - Crystal Melting, Academic Press, New York, 1980.
20. F. Franks. *Process Biochem.* 24(1), R3-R7 (1989).
21. H. Levine and L. Slade, in *Water and Food Quality*, ed. T.M. Hardman, Elsevier Science, London, 1989, pp. 71-134.
22. J.D. Ferry, *Viscoelastic Properties of Polymers*, 3rd edn., John Wiley & Sons, New York, 1980.
23. L.H. Sperling, *Introduction to Physical Polymer Science*, Wiley-Interscience, New York, 1986.
24. D. Simatos and M. Karel, in *Food Preservation by Moisture Control*, ed. C.C. Seow, Elsevier Applied Science, London, 1988, pp. 1-41.
25. L. Slade, H. Levine and J.W. Finley, in *Protein Quality and the Effects of Processing*, ed. D. Phillips and J.W. Finley, Marcel Dekker, New York, 1989, pp. 9-124.
26. H. Levine and L. Slade, in *Dough Rheology and Baked Product Texture: Theory and Practice*, ed. H. Faridi and J.M. Faubion, Van Nostrand Reinhold/AVI, New York, 1989, pp. 157-330.
27. R.K. Chan, K. Pathmanathan and G.P. Johari. *J. Phys. Chem.* 90, 6358-6362 (1986).
28. W.M. Nicol, in *Sugar: Science and Technology*, ed. G.G. Birch and K.J. Parker, Applied Science, London, 1979, pp. 211-230.
29. A.P. MacKenzie. *Phil. Trans. Roy. Soc. Lond. B.* 278, 167-189 (1977).
30. J.M.V. Blanshard and F. Franks, in *Food Structure and Behaviour*, ed. J.M.V. Blanshard and P. Lillford, Academic Press, London, 1987, pp. 51-65.
31. E. Mayer. *Cryo-Lett.* 9, 66-77 (1988).
32. T. Soesanto and M.C. Williams. *J. Phys. Chem.* 85, 3338-3341 (1981).
33. M. Karel. Personal communication (1988).
34. C.Y. Lee, N.L. Smith and D.E. Hawbecker. *J. Food Qual.* 11, 279-287 (1988).
35. R. Duden and A. Scholz. *Z. Ernährungswiss.* 21, 266-271 (1982).
36. E.L. LeBlanc, R.J. LeBlanc and I.E. Blum. *J. Food Sci.* 53, 328-340 (1988).
37. J.G. Morris, *A Biologist's Physical Chemistry*, Edward Arnold, London, 1968.
38. P. Baardseth and E. Naeset. *Food Chem.* 32, 39-46 (1989).
39. C.A. Angell. *Ann. Rev. Phys. Chem.* 34, 593-630 (1983).
40. K. Hofer, A. Hallbrucker, E. Mayer and G.P. Johari. *J. Phys. Chem.* 93,

4674-4677 (1989).

41. C.A. Angell, E.J. Sare, J. Donnelly and D.R. MacFarlane. J. Phys. Chem. 85, 1461-1464 (1981).
42. M. Forsyth and D.R. MacFarlane. Cryo-Lett. 7, 367-378 (1986).
43. F. Franks, Biophysics and biochemistry at low temperatures, Cambridge University Press, Cambridge, 1985.
44. F. Franks, in Biophysics of Water, ed. F. Franks, John Wiley & Sons, New York, 1982, pp. 279-294.

A) DSC

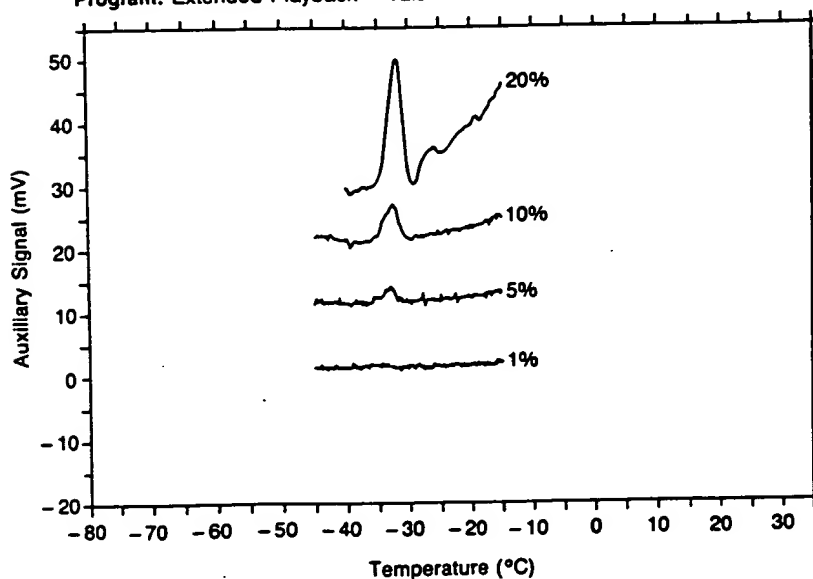
Sample: 20% SUCROSE
Size: 7.41 MG
Rate: 5 DEG/MIN
Program: Extended Playback V2.0



DuPont 1090

B) DSC

Sample: SUCROSE
Size: 2.39 MG
Rate: 5.0 DEG/MIN -70 TO +40
Program: Extended Playback V2.0

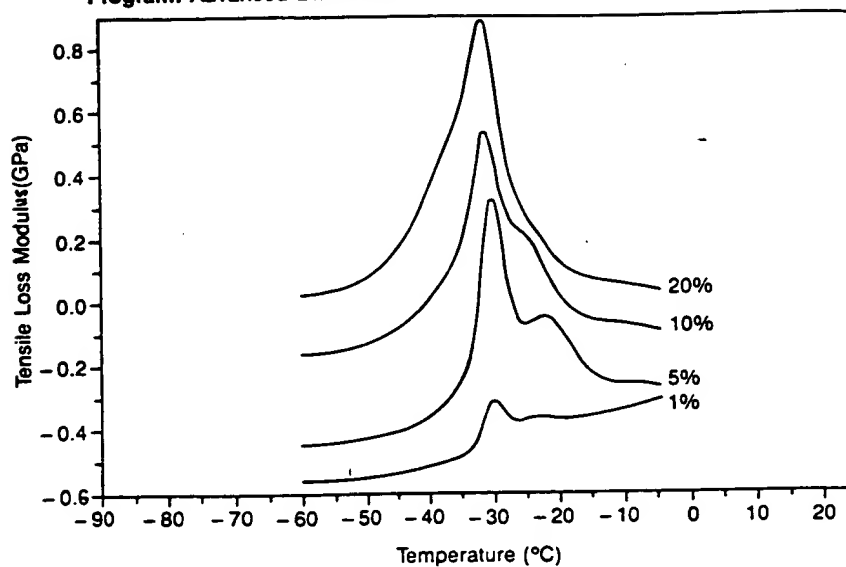


DuPont 1090

Figure 1. A) DuPont 1090 DSC primary heat flow curve (endo down) and auxiliary digital derivative profile (endo up) for 20 w% sucrose solution; B) DuPont 1090 DSC digital derivative profiles for 20, 10, 5, and 1 w% sucrose solutions. Reproduced, with permission, from (6).

C) DMA

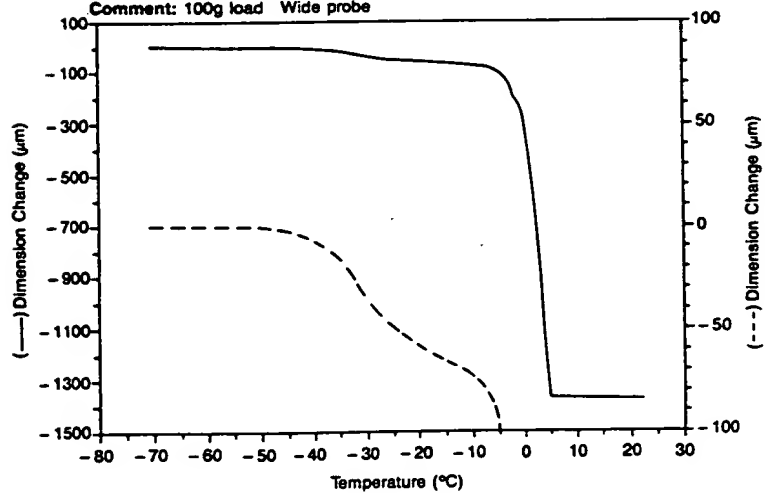
Sample: SUCROSE
Size: 12.32x11.14x1.54 MM
Rate: 5 DEG/MIN -60 TO +25
Program: Advanced DMA V1.0



DuPont 1090

D) TMA

Sample: 20% SUCROSE
Size: 1.40 mm
Method: Softening Profile-5
Comment: 100g load Wide probe



DuPont 9900

Figure 1. C) DuPont 981 DMA loss modulus curves for 20, 10, 5, and 1 w% sucrose solutions; D) DuPont 943 TMA curve of dimension change vs. temperature for 20 w% sucrose solution. Reproduced, with permission, from (6).

Figure 2. Schematic state diagram of temperature vs. weight percent solute for an aqueous solution of a hypothetical small carbohydrate (representing a model frozen food system). Various cooling/heating paths and associated thermal transitions measurable by low-temperature differential scanning calorimetry are illustrated relative to the glass, liquidus, and devitrification (T_d) curves. Reproduced, with permission, from (7).

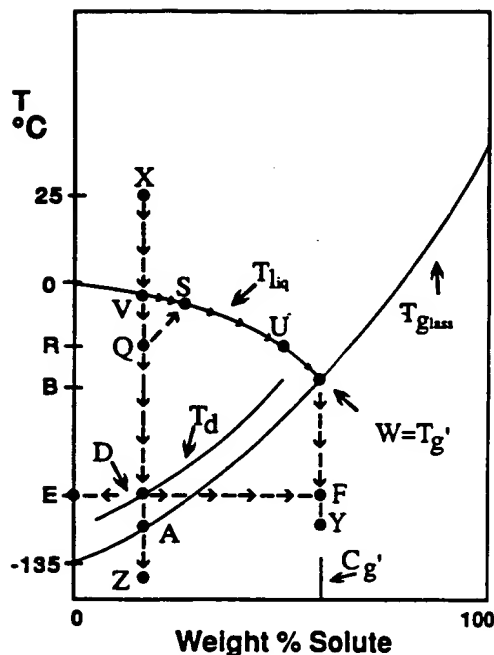


Figure 3. Dynamics map (equilibrium and non-equilibrium state diagram) for the sucrose-water system. The locations of the glass, liquidus, and solidus curves are shown with their respective points of intersection: T_g' at the intersection of the glass curve and non-equilibrium extension of the liquidus curve and T_e (eutectic melting temperature) at the intersection of the liquidus and solidus curves. The curve for the vaporization temperature of water as a function of sucrose concentration (28) is included. Reproduced, with permission, from (7).

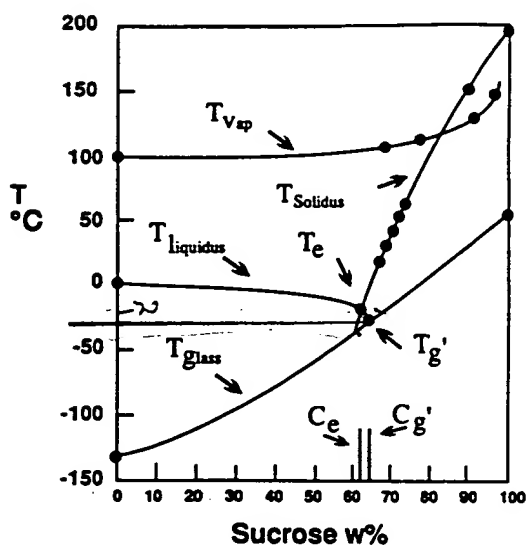


Figure 4. Schematic dynamics map to illustrate the relative magnitudes of the temperature range, $\Delta T = T_m - T_g$, corresponding to the region of WLF kinetics. Relative magnitudes of the temperature range corresponding to the WLF rubbery region are emphasized by dark bars for pure solute, pure water, and the freeze-concentrated matrix of amorphous solute-unfrozen water as it exists between the eutectic melting temperature and T_g' . Reproduced, with permission, from (6).

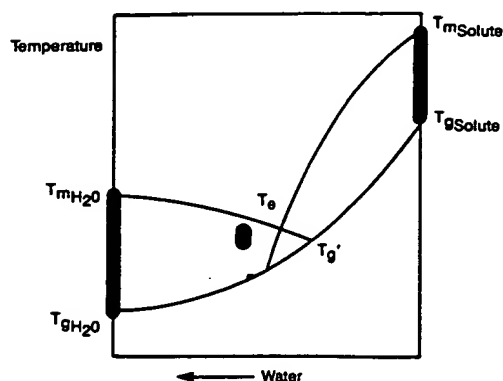


Figure 5. WLF plots of freezer-storage stability of organoleptic quality for experimental a) ice cream products and b) frozen novelties. Log [iciness score] is plotted as a function of ΔT ($= T_f - T_g'$). Iciness score was determined organoleptically, on a 0-10 point scale, after 2 weeks of deliberately abusive (temperature-cycled) frozen storage in a so-called "Brazilian Ice Box". [The straight dashed line drawn in part (b) represents the behavior expected for Arrhenius kinetics with temperature dependence corresponding to $Q_{10} = 2$.] Reproduced, with permission, from (6).

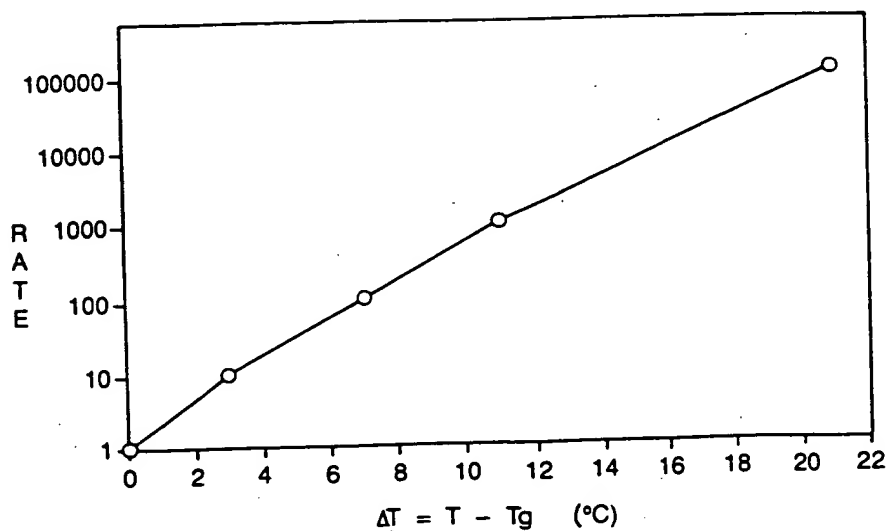
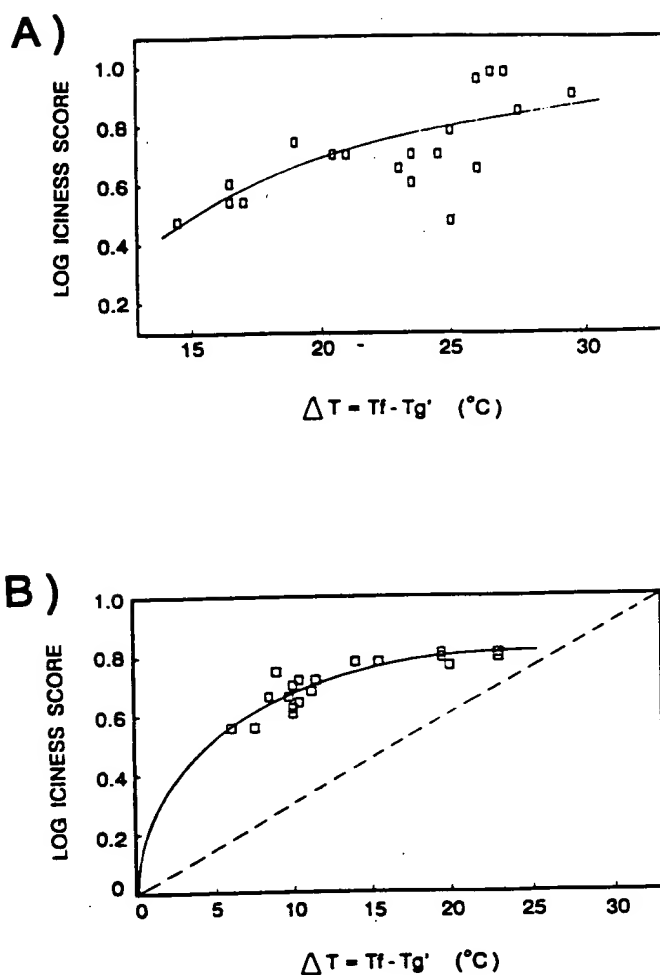


Figure 6. Variation of the relative rates of a diffusion-limited relaxation process with $\Delta T = T - T_g$, as defined by the WLF equation with the "universal" constants of $C_1 = 17.44$ and $C_2 = 51.6$, typical of "well-behaved" synthetic polymers, food solutes, and concentrated aqueous solutions, alike. Reproduced, with permission, from (6).

A hand-drawn diagram of a circle, possibly representing a celestial body or a cross-section. The circle is divided by several intersecting lines. In the upper right quadrant, there are two rectangular boxes, each containing the number "060". Below them is a circular shape containing the number "130". To the left of these, there are handwritten numbers "370" and "340". In the lower right quadrant, the word "Ref." is written vertically. Below it, the number "800" is written, followed by "500" and "200". At the bottom center, there is a small arc labeled "11". On the left side, there is a curved arrow pointing downwards and to the left. The entire diagram is drawn with dark ink on a white background.

Joe

334

۱۲

Joe

10

John Wiley & Sons, Limited, Chichester
: Akadémiai Kiadó, Budapest

continues, possibly over many years. This type of approach is expensive, both in time and resources, but is not surprising when the consensus of opinion from experts in the field can be expressed as 'Freezing and drying data can only be determined empirically by the trial and error method i.e. by way of testing the finished product' [1].

The quality of a product

The quality of a freeze-dried product (Fig. 1A) is assessed by its shelf-life, rehydratability and activity although secondary features such as appearance cannot be overlooked. These quality features are related back to the moisture content of the product throughout processing. Moisture content is in turn dependent on the settings of the process parameters that can be controlled in the freeze-dryer; temperature, pressure and time. We have considered the biophysical processes that underlie freeze-drying (Fig. 1B). Although all the factors need to be taken into account when determining an optimum freeze-drying cycle, probably the most important is vitrification.

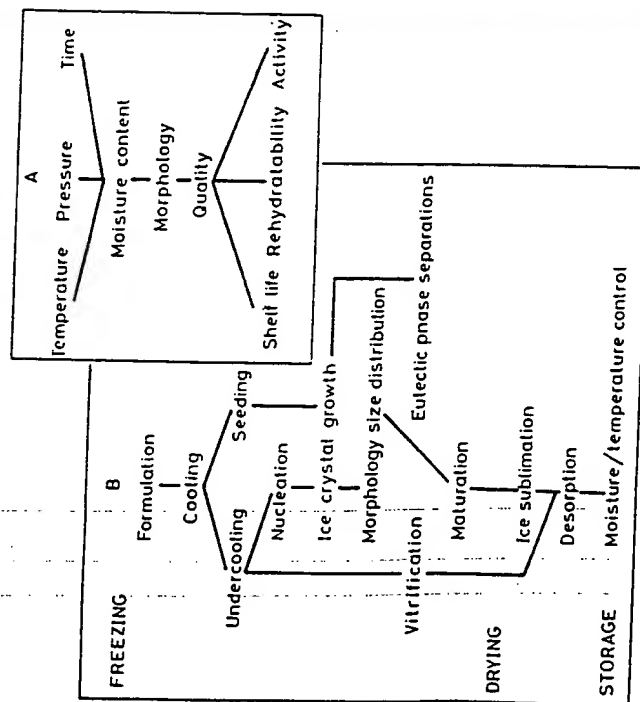


Fig. 1 (A) Experimental variables which determine the quality of the product. (B) Physical parameters that influence freezing and drying behaviour (Taken from reference 2)

Vitrification and freeze-drying

Figure 2 shows a plot of temperature against mol fraction of solids, in this case sucrose. Depending on starting concentration, two possible situations can arise on cooling. In dilute solutions (e.g. 40% by weight sucrose) ice will form as the temperature is reduced to below the liquidus curve. This will result in a two phase system consisting of pure ice and a freeze concentrate (solid and unfrozen water). As the temperature is further reduced more ice will crystallize and the freeze concentrate will be further concentrated. Eventually the freeze concentrate will become so concentrated (for sucrose circa 80 weight percent) that it will undergo a sharp increase in viscosity and form a glass – that is, it will vitrify. The temperature at which this glass transition takes place is termed T_g . In solutions that are initially highly concentrated (e.g. sucrose >80% by weight) freezing will not occur and on cooling, the preparation will form first a rubber and then a glass.

Freeze drying starts with a dilute solution. As described for dilute solutions, on cooling ice crystallizes out, resulting in a concentration of the remaining material. With further reductions in temperatures more ice crystallizes and the material becomes more and more concentrated until it forms a glass at T_g , the temperature of maximum freeze concentration where the viscosity is such that no more ice can form. Under such conditions any labile

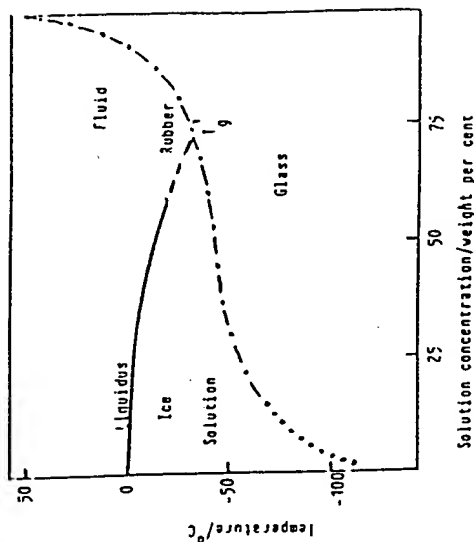


Fig. 2 State diagram for the binary system sucrose + water, showing the equilibrium liquidus and the non-equilibrium glass transition curve: all points on this curve have the same viscosity

material that was in the preparation (e.g. enzyme) will be trapped in the glass and effectively stabilized by immobilization.

In freeze-drying the ice phase is next removed by sublimation (primary drying). In order to protect the protein as described above this must be performed at a temperature $< T_g$. Knowing the rate of ice sublimation at T_g the duration of this stage of processing can be calculated. At the end of primary drying the remaining material is an amorphous glass containing typically 30 weight percent water. This is then heated and further water removed (secondary drying). For this stage, the rate of temperature increase and duration of processing can be calculated from the rate of diffusion of the residual moisture from the partially dried matrix. At the end of secondary drying the product has a low moisture content and an enhanced T_g . Provided the material is then stored below T_g in a glassy state, its stability should be maintained.

A predictive approach to freeze drying

There are three measurements that provide sufficient information that a predictive model of an optimum freeze-drying cycle can be produced. They are, the temperature of maximal freeze concentration, (T_g'), the amount of unfrozen water at this temperature (W_g') and T_g of the dried product, the latter providing critical information on the quality and storage stability of Differential scanning calorimetry (DSC).

If a typical solution, as used in freeze-drying, is cooled to some subzero temperature, a DSC trace as shown in Fig. 3 is obtained upon reheating. The area under the endotherm corresponds to the melting of ice. From the area amount of frozen water in the sample can be calculated. Since, the initial amount of water and solid in the sample is known, W_g' (the amount of unfrozen water at T_g') can be derived. This is the mass of water that has to be removed during secondary drying. It is also possible to determine T_g' by measuring the peak areas and melting temperatures for a range of different solid water ratios and extrapolating back to zero frozen water, i.e. T_g . This is time consuming and prone to errors in area measurements due to difficulty in accurately determining the baseline for an area measurement, especially at low water concentration. A better method is to determine T_g' directly.

Computers provide an ideal tool to do this, enabling among a number of things the capability to zoom in on sections of the curve and analyse them in detail. If we do this here we find the second order glass/rubber transition associated with T_g (Fig. 3).

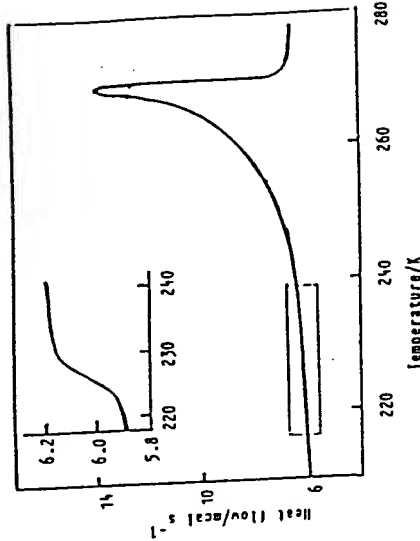


Fig. 3 The complete melting trace of a frozen sucrose solution subject to a typical freeze-thaw process. Inset is an expansion of the area in the rectangle. The glass transition at 227 K can be clearly seen

However, the relative magnitudes of the small glass transition to the large melting peak often results in the obliteration of the lower transition by the 'correction' software. Our system (DARES-DSC) has been reported in detail elsewhere [3], its main features are listed in Table 1.

The third variable that can be measured in the glass transition temperature of the dried product. On first heating a characteristic glass transition temperature with some relaxation is observed. On the second run the relaxation is removed. Sometimes, as is the case in Fig. 4, the relaxation can be deceptive so care needs to be taken and at least two runs made. Figure 4, shows a plot of heat flow vs. temperature for freeze-dried product. The first scan, if seen in isolation, would appear to be the first order endothermic transition. In this case it could not be, as the material was a pure sucrose glass. If the sucrose had crystallized, a melt would be expected above 420 K. The second run confirmed this, showing T_g at the same temperature as the thermal event obtained on the first run. The first run is therefore a glass temperature with an extremely high degree of relaxation.

Table 1 Major features available within the DARES-DSC program [3]: selection is from menus with the aid of a mouse

Visual aids	Calculations	Output facilities	Input/edit facilities
Extrapolate line Scale display Mark transition temperature Overlay traces Level trace	Area calculation Transition temperature Slope gradient Differentiate (any order) Subtract traces Average traces Divide traces	Print graph as displayed Print-out of data Output to disk as ASCII file Print index of disk contents Backup disk Delete files Write calorimeter data to disk Write edited data to disk	Take data from calorimeter Input stored file from disk Edit user variable fields

The importance of the measured variables in freeze-drying

During primary drying the sample must be kept below T_g so that the enzyme is stabilized in an amorphous glass and protected from damage. If the product temperature is allowed to rise above T_g then some of the ice will melt back into the non-ice phase forming a highly concentrated solution.

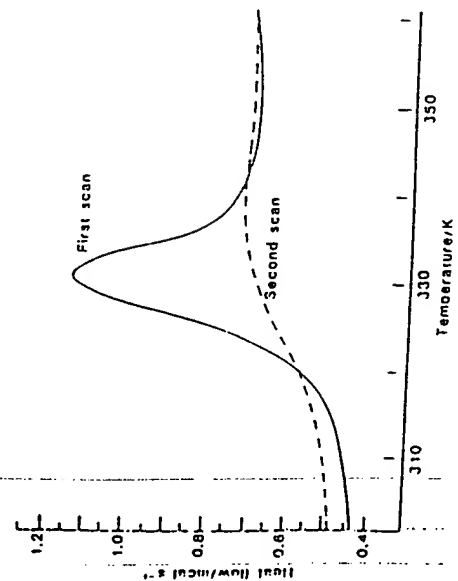


Fig. 4 The overlaid traces obtained on the first and second heating scans of a freeze-dried product that is expected to show a second order (glass) transition. The implications are discussed in the text

Under these conditions the enzyme will be prone to inactivation and the product matrix in danger of collapse due to a weakening of its structure. Since ice sublimation rates are much more rapid at higher temperatures, it is desirable that the products to be freeze-dried have a high T_g . The addition of stabilizers that themselves have high T_g 's is preferred since these will raise the T_g of the preparation as a whole. A list of possible stabilizers is shown in Table 2. It can be seen that materials such as maltotriose ($T_g = 249.5$ K) can be used. Glycerol is unfavourable because it has a low T_g . In general it can be considered that low molecular weight species (e. g. salts) will suppress T_g while large molecules, e. g. carbohydrates and, very often, the active material itself, will raise T_g . The overall T_g of a preparation will be related to the mass ratio of the solid components.

Table 2 Glass/rubber transitions of anhydrous (T_g) and freeze-concentrated (T_g') carbohydrates and water contents of the freeze-concentrates. Data from Ref. [4, 5]

	T_g , K	T_g' , K	wt% water
glycerol	180	208	46
xyliol	234	226.5	42.9
ribose	263	226	33
xylose	282	225	31
glucitol (sorbitol)	270	229.5	18.7
glucose	312	230	29.1
mannose	303	232	25.9
galactose		232.5	45
fructose	286	231	49
maltose	316	243.5	20
cellobiose	350		
trehalose	350	243.5	16.7
sucrose	330	241	35.9
glucose/fructose (equimolar)	293	230.5	48
maltotriose	349	249.5	31

W_g is the amount of water that needs to be removed during secondary drying. This should be as low as possible because it then enables a more rapid secondary drying. A low W_g also reduces the probability of product collapse. Combining T_g and W_g requirement, the best types of stabilizers are those such as maltose and sucrose. Sucrose has a further advantage in that it is inexpensive.



Fig. 5 Scanning electron micrographs of freeze-dried therapeutic products which had been frozen to -50°C . Sample (a) had a $T_g > -50^{\circ}\text{C}$ and (b) a $T_g < -50^{\circ}\text{C}$. The structure of the freeze-dried (b) is poor due to incomplete freeze concentration during primary drying.

The T_g value of the dried product gives the maximal safe storage temperature. If kept below T_g , the enzyme will be in an amorphous glass, physically protected from decay. If stored for extended periods above this temperature, it is prone to activity loss.

An example of the importance of T_g in a real situation

The product was a mixture of protein, sucrose and salt. It was routinely frozen to -50°C then freeze-dried. However, there was a marked variance in batch quality. Figure 5a shows an electron micrograph of a good product, the open structure indicates good drying. Following indifferent drying, the open structure is lost (Fig. 5b). This product is difficult to rehydrate and has poor stability. The only difference in the formulation and processing specifications between the batches was the protein content. We examined both a high and low protein concentration preparation. The former has a T_g of 226 K (Fig. 6a), that is, above the freezing temperature of -50°C . The product should be stable during primary drying since the active protein will be 'trapped' in a glass. The low protein preparation had T_g below the freezing temperature (Fig. 6) and therefore was still in a rubbery state during primary drying. This resulted in partial collapse during processing, giving a poor product.

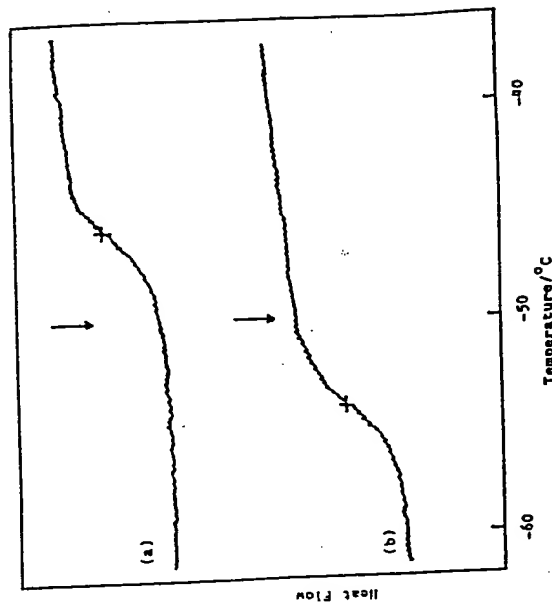


Fig. 6 DSC heating scans of the preparations shown in Fig. 5. The routine freezing temperature is indicated by the arrows and T_g by +. The two preparations differ only in the protein concentration of the solutions. The sample with the lowest protein concentration has the lowest T_g .

In order to ensure that the product is of a constant high quality, regardless of protein concentration, it must be ensured that the product is always in the

form of a glass during primary drying; it must always be frozen to below T_g . There are a number of ways of doing this but probably the most effective is to compensate for the drop in T_g caused by the reduction in protein concentration by adding extra sucrose.

Conclusion

DSC can be used to measure the physical constants that are important for freeze-drying. These measurements can then be used to define the optimum processing parameters – time, temperature and pressure. This approach is more efficient in terms of time and cost than deriving the process parameters by trial and error. Additionally, the measurement of T_g of the dried product gives an immediate indication, directly after the completion of processing, as to its long-term stability. A more detailed discussion of how the concepts reported here can be used to improve freeze-drying is given in references 2 and 6.

References

- 1 H. Willemer, Joint Meeting IIR Commission C1 and C2 Karlsruhe (1977) 1.
- 2 P. Franks, *Cryo-Letters*, 11 (1990) 93.
- 3 R. H. M. Hatley, P. Franks and M. Green, *Thermochim. Acta*, 156 (1989) 247.
- 4 H. Levine and L. Slade, *Pure and Appl. Chem.*, 60 (1988) 1841.
- 5 H. Levine and L. Slade, *Cryo-Letters*, 9 (1988) 21.
- 5 L. X. Finegold, P. Franks and R. H. M. Hatley, *J. Chem. Soc. Faraday Trans. 1* 20 (1989) 2945.
- 6 P. Franks, *Process Biochem.*, Feb. 1989 Supplement.

Zusammenfassung – Die Eigenschaften und die Stabilität proteinhaltiger Produkte im gefriergetrockneten Zustand sind durch die gewählten Prozessbedingungen und durch die physikalischen Eigenschaften der Endprodukte vorgegeben. Insbesondere sind die Glasumwandlungstemperaturen des Gefrierkonzentrates und des getrockneten Produktes als auch der endgültige Wassergehalt von Bedeutung. In der vorliegenden Arbeit werden DSC-Untersuchungen zur Optimierung des Gefrierkonzentrationsprozesses als auch Studien zur Stabilität der Produkte dargestellt.

Organic Chemistry

DETERMINATION OF KINETIC MODELS BY THE USE OF PATTERN RECOGNITION METHODS

E. Koch

MAX-PLANCK-INSTITUT FÜR STRACHIELENCHEMIE, STIFTSTR. 34-36, 4330 MÜLHEIM A. D. RUHR, GERMANY

Thermoanalytical records obtained in homogeneous systems can be interpreted kinetically by the study of information strings, based on the type of concentration dependence of the mechanistic coordinates, shape index and reaction type index (as the signal height or reciprocal halfwidth referred to unit concentration and activation data [1, 2]). These are available experimentally (ca. 3000 DTA and UV plots were studied) and theoretically, using a Gear integration subroutine as a component of an expert system [2].

A prerequisite for the reliable function of this comparing strategy is the existence of a THEOREM OF COMMON KINETIC RUNS, which means that for a definite model such as 'Mechanistic Concentration Code' (= MCC; [3]) does not depend on the activation data or the signal parameters of the steps (proportionality coefficients, as reaction enthalpy for DSC or DTA). Recently it could be revealed that the MCC-strings of all two-step models consist of independent main parts (i.e., first and last element = orders of reference step or the other step, respectively, and 'sign' elements, + or -, between) and parts beside which are partially dependent on signal parameters or, less, activation parameters; however, application of the probability theory confirms [4, 5] that the deviations of individual total strings from the source strings usually do not exceed 10%.

This means reliable kinetic equivalence of different methods and indicates a fundamental pathway to a systematic model search, based on the reaction matrix of the ODE system, which should be probably transferable to heterogeneous kinetics. In this case, the serious problem of the reliability of

**This Page is Inserted by IFW Indexing and Scanning
Operations and is not part of the Official Record**

BEST AVAILABLE IMAGES

Defective images within this document are accurate representations of the original documents submitted by the applicant.

Defects in the images include but are not limited to the items checked:

- ☒ **BLACK BORDERS**
- ☐ **IMAGE CUT OFF AT TOP, BOTTOM OR SIDES**
- ☐ **FADED TEXT OR DRAWING**
- ☐ **BLURRED OR ILLEGIBLE TEXT OR DRAWING**
- ☐ **SKEWED/SLANTED IMAGES**
- ☐ **COLOR OR BLACK AND WHITE PHOTOGRAPHS**
- ☐ **GRAY SCALE DOCUMENTS**
- ☐ **LINES OR MARKS ON ORIGINAL DOCUMENT**
- ☐ **REFERENCE(S) OR EXHIBIT(S) SUBMITTED ARE POOR QUALITY**
- ☐ **OTHER:** _____

IMAGES ARE BEST AVAILABLE COPY.

As rescanning these documents will not correct the image problems checked, please do not report these problems to the IFW Image Problem Mailbox.